Semnan University

Progress in Physics of Applied Materials

journal homepage: https://ppam.semnan.ac.ir/

Influence of Temperature Dependence of Electrical Conductivity of Graphite Crucible in Czochralski Crystal Growth: A Numerical Analysis

Sanaz Hadidchi, Mohammad Hossein Tavakoli*

Physics Department, Bu-Ali Sina University, Hamedan 65174, I.R. Iran

ARTICLE INFO

Article history:
Received: 5 December 2023
Revised: 17 December 2023
Accepted: 23 December 2023

Keywords:
Czochralski
Induction heating
Electromagnetic wave
Electrical conductivity

ABSTRACT

Graphite crucibles are widely used in induced crystal growth systems. This study examines the impact of temperature variation on the electrical conductivity of the graphite crucible and its influence on the temperature field and melt flow in a Czochralski germanium crystal growth furnace using the two-dimensional finite element method. The in-depth analysis demonstrates that the temperature-dependence of electrical conductivity of the crucible is crucial in the growth process and the thermal field of the setup. Specifically, it is noted that temperature changes have a significant effect on the generation and distribution of induction heat, the temperature and melt flow field, the complex shape of the crystal-melt interface, as well as the stress and dislocations in the grown crystal. These findings highlight the intricate relationship between temperature, crucible conductivity, and the dynamics of the crystal growth process, providing insight into the subtle factors that impact the quality and properties of the resulting crystal.

1. Introduction

The Czochralski (CZ) method is a crystal growth technology that involves placing a small seed crystal into a melt and pulling it upwards under specific conditions to obtain a single crystal. This technique is widely used today to produce single crystals of materials such as Si and Ge.

The crucible used in the Czochralski method is typically heated in two ways: resistive heating and induced heating. Induced heating has several advantages, including rapid and consistent heating, precise and repeatable production rates, and clean, contamination-free processes. Graphite is a popular material used as a crucible in the growth process. Its popularity stems from its thermal conductivity, resistance to high temperatures and low coefficient of thermal expansion for high-temperature applications, anti-strain properties for rapid heating and cooling, resistance to corrosion from acids and alkaline solutions, and excellent chemical stability. Graphite crucibles are non-reactive and can remain intact at very high temperatures.

In order to create a melt, it is necessary for the crucible to endure burning and heating without harm. The prevalent utilization of graphite crucibles calls for a deeper comprehension of their characteristics, particularly their electrical conductivity. The shape, size, and temperature of a crucible all have an impact on its electrical conductivity. The conductivity properties of conductors and semiconductors differ when subjected to heat and temperature fluctuations. While the conductivity of a conductor diminishes when heated, the electrical conductivity of a semiconductor increases with temperature, leading to a decrease in resistance.

Graphite, a non-metallic conductor, can easily conduct electricity due to the presence of electrons between its carbon atom layers [1]. However, during growth, the conductivity of the graphite crucible decreases significantly when heated above the melting point of germanium (1210 K) [2]. The conductivity of the graphite crucible is approximately 7×104 S/m at room temperature, but it decreases to about 151 S/m when heated, as shown in Figure 1. Therefore, it is important to investigate the significant temperature effect on the electrical conductivity of the graphite crucible in relation to the crystal growth process.

* Corresponding author.
E-mail address: mhtvkl@gmail.com

Cite this article as:
Hadidchi S., Tavakoli M.H., 2023. Influence of Temperature Dependence of Electrical Conductivity of Graphite Crucible in Czochralski Crystal Growth: A Numerical Analysis. *Progress in Physics of Applied Materials*, 3(2), pp. 131-139. DOI: 10.22075/PPAM.2023.32556.1073

Extensive research has been conducted on induced heating and related phenomena in crystal growth using the Czochralski method. Numerical methods [3-6] and various software packages such as Comsol, Elmer, etc. [7], as well as experimental studies [8], have been used for this purpose. This paper aims to simulate and investigate the impact of varying electrical conductivity of the graphite crucible with temperature on the induction heating process, temperature field, and melt flow in the CZ-Ge growth system using the Comsol software package.

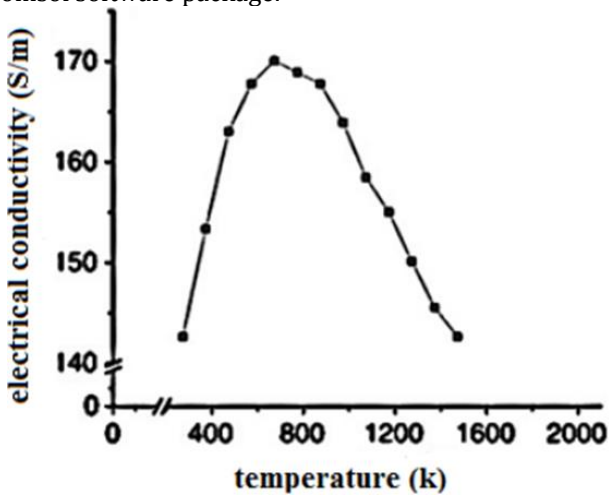

Fig. 1. Electrical conductivity of graphite as a function of temperature [2].

2. Modeling

The germanium Czochralski crystal growth system consists of various components: an RF copper coil, a graphite crucible, a quartz seed holder, and a stainless steel chamber with circulating water. The furnace chamber is filled with argon gas. Figure 2 depicts the computational domain and related meshing. Assuming axial symmetry and a fully symmetric furnace geometry with respect to the central axis, numerical modeling of crystal growth is conducted. An eight-loop inductor wire induction coil with a frequency of 32 kHz is utilized, and the growth process is assumed to be nearly steady-state. The electrical conductivity of graphite is considered at both room temperature and the melting temperature of germanium. The thermal and physical properties used in Table 1 and operational parameters presented in Table 2.

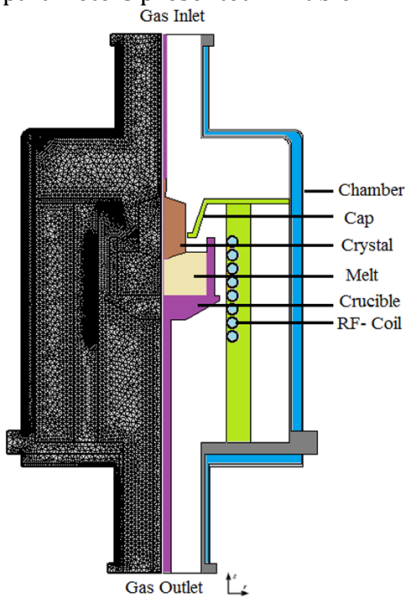

Fig. 2. CZ growth system of germanium crystal and its computational mesh.

Table 1. Physical Properties of Materials [3 and 9, 10].

Material	Density (ρ)	Specific Heat Capacity (C_p)	Electrical Conductivity (σ_{el})
	(kg/m^3)	(J kg^{-1} K^{-1})	(S/m)
Stainless Steel	7850	475	1.00×10^6
Graphite	1800	710	-
Quartz	2650	730	1
germanium (melt)	5323	310	2.00×10^6
germanium (crystal)	5320	322	2.00×10^6
Copper	8960	385	6.00×10^7
Alumina	3900	900	1×10^{-18}

Our mathematical model of induction heating has been described in detail elsewhere [10].

Here, we describe the thermal and heat transfer modeling. The Navier-Stokes equations and continuity equation are expressed as the governing equations for heat transfer [10,11]:

$$\rho\left(\vec{V}.\vec{\nabla}\right)\vec{V} = -\vec{\nabla}p + \mu\nabla^2\vec{V} + \rho\vec{g}\beta\left(T - T_0\right) \quad (1)$$

$$\nabla.\vec{V} = 0 \quad (2)$$

Where β, ρ, and μ represent the volumetric thermal expansion coefficient, density, and dynamic viscosity of the fluids, respectively. T is the temperature, and T_0 is the reference temperature typically set at 300 Kelvin. $\vec{V}$ is the velocity vector, and $\vec{g}$ is the gravitational acceleration vector.

Table 2. Operational Parameters of the Growth System

Parameter	Value
Crucible Radius (mm)	90
Crucible Height (mm)	90
Crystal Radius (mm)	45
Crystal Rotation Rate (rpm)	-15
Crucible Rotation Rate (rpm)	5
Pulling Rate (mm/h)	1
Argon Flow Rate (lit/min)	1

The energy equation for heat transfer is defined as follows:

$$\alpha\nabla^2 T - \vec{V}.\vec{\nabla}T + q = 0, \quad (3)$$

In a place where α is the thermal diffusivity coefficient, equal to k/ρC, where k and C are the thermal conductivity and specific heat of the material, respectively. The heat source parameter, generated by electromagnetic induction through high-frequency current, is represented by q. Since magnetic insulation boundary conditions are used at the domain boundaries to calculate the magnetic field, the simulation domain should be sufficiently large. Water cools the internal walls of the chamber and the coils, and for this reason, the temperature at the coil and the water-chamber interface is set to 300 Kelvin. In the solid/liquid interface, the latent heat of fusion is released.

$$k_l \frac{\partial T_l}{\partial \vec{n}} - k_s \frac{\partial T_s}{\partial \vec{n}} = -\rho_s H_f \vec{V}_{\text{pulling}} \quad (4)$$

This represents the overall heat flow balance. $\vec{n}$ is the unit vector in the normal direction in the common phase, l and s represent the liquid (melt) and solid (crystal) phases respectively, Hf (465 kJ/kg) is the latent heat of crystallization, and $\vec{V}_{\text{pulling}}$ pulling is the crystal growth rate along the axis. The heat balance equation in the inner surfaces of the furnace is as follows:

$$-k_i \frac{\partial T_i}{\partial \vec{n}} = \sigma\varepsilon_i (T_i^4 - T_a^4)\vec{n}, \quad (5)$$

Where, the indices i and a indicate any level that is in contact with the gas and fluid environment surrounding the surface. The boundary conditions without slip occur on all interfaces of the furnace elements with gas, melt/crystal, and melt/wall interfaces. Since the crystal is growing and the melt is rotating during the process, the velocity on the common solid/liquid surface is given by $v_x = r\omega_x$ for the crystal and $v_c = r\omega_c$ for the melt, where ω_x and ω_c are the respective rotation rates of the crystal and melt. The vector component of the fluid velocity $\vec{V}$ = (u, *v*, w), *v* is vertical, and r represents the radial position of the crystal or melt.

Argon gas and germanium melt are immiscible fluids, so the vertical component of the flow (w) is zero at the free surface, and the thermocapillary effect induces flow from the cold point to the hot point in the gas/melt common region.

$$\mu_l \frac{\partial u_l}{\partial \vec{n}} - \mu_g \frac{\partial u_g}{\partial \vec{n}} = \frac{\partial \gamma}{\partial \vec{\tau}} = \frac{\partial \gamma}{\partial T}\frac{\partial T}{\partial \vec{\tau}} \quad (6)$$

The place where $\partial\gamma/\partial\vec{\tau}$ has a tangential coefficient of 7.32×10^{-5} (N/m K) and the index g is related to the gas. $\vec{\tau}$ is the unit tangent vector on the common surface, and u is the radial velocity.

Thermal stress equation in the crystal has been described in detail elsewhere [11] and dislocation density n_{disl} in the grown crystal is calculated by $n_{disl} = \frac{\alpha}{b}\frac{\partial T}{\partial r}$, where $\frac{\partial T}{\partial r}$ is the radial temperature gradient [16]. The a/b ratio for germanium crystal is equal to 15300 m/K.

The FEM grid (Figure 2) is designed to accurately represent the crystal geometry and the surrounding environment. The grid will be finer in regions where detailed information is required, such as near crystal-gas, crystal-melt, and melt-gas interfaces, and coarser in regions where less detail is required.

3. Results and discussion

In this study, we examine the effect of temperature-dependent electrical conductivity of the crucible on the thermal field of the growth system, melt convection, and thermal stress in the grown crystal.

In the process of melting germanium powder at 1210 K, the electrical conductivity of the crucible changes with the rising temperature. We will consider two cases for the electrical conductivity of the graphite crucible: Case 1: at room temperature (70,000 S/m) Case 2: at the melting point of germanium (151 S/m).

As the temperature rises, the crucible's conductivity decreases, resulting in an increase in its electrical resistance. This impacts the penetration depth through changes in three parameters (Equation 7) [12-16]: frequency variation (a wide range of different RF frequencies are generated), permeability variation (changes in the crucible material), and variation in electrical conductivity.

$$\delta = \sqrt{\frac{1}{\pi\mu\sigma f}} \quad (7)$$

Table 2 displays the operational parameters for computations. All calculations are performed with a one-centimeter crystal, a crystal pulling rate of 1 millimeter per hour, a flow rate of 1 liter per minute of argon gas, and crystal and crucible rotation rates of 15 and 5 revolutions per minute, respectively. The frequency of the RF-coil is denoted as f (32 kHz), while the specific electrical conductivity and magnetic permeability are denoted as σ and μ, respectively. The skin depth, which is the distance from the surface of an object to the depth at which the electromagnetic field and current intensity decrease to 37% of their surface values, increases as electrical conductivity decreases. There is an inverse relationship between skin depth and electrical conductivity. The presence of a graphite crucible containing molten material impedes the penetration of electromagnetic waves generated by the RF-coil. The electrical conductivity of the crucible affects the penetration of electromagnetic waves into the crucible and melt, as well as the heat generated in them. The crucible,

acting as a barrier to electromagnetic energy at a specific frequency, reflects, absorbs, and scatters some of the waves when electromagnetic waves collide with their surface. The remaining waves are transmitted through the crucible. The presence of electrical conductivity and magnetic permeability in the crucible results in protective mechanisms of reflection and absorption.

3.1. Inductive Heating

During the process of induction heating, the Graphite crucible plays a critical role in the distribution and transfer of heat. The crucible's conductivity directly impacts the distribution of electrical current and, consequently, the distribution of inductive heating in the system. Figure 3 illustrates the heat distribution generated in the system. The RF-coil's electromagnetic waves are unable to penetrate the molten material because of the crucible's presence. Furthermore, the heat generated in the system is concentrated in a thin layer on the crucible's surface, a result of the skin effect. As the crucible's conductivity increases, the distribution of induction heating in the system improves, leading to a more uniform temperature on the crucible's surface.

Table 3 presents data on the current intensity and heat produced for each case. At high temperatures, the total heat generated increases as the crucible conductivity decreases, due to the higher input electrical current to the coil. In the growth system, a higher input electric current is needed to maintain a constant diameter of the Ge crystal as the crucible conductivity decreases. In Case 1, the lower conductivity of the crucible leads to a reduced penetration depth of the electromagnetic field into the molten material, resulting in less heat generation. However, the heat generated in the crucible is higher due to the lower penetration depth.

In Case 2, the inductive heating distribution extends from the outer surface of the crucible to its inner part as penetration depth increases and conductivity decreases. This results in a stronger electromagnetic field within the molten material, leading to more heat in the melt and less heat generation in the crucible. Consequently, the electrical conductivity of the crucible directly impacts the production and distribution of induction heating in the growth furnace. Enhancing the electrical conductivity of the crucible can boost inductive power and enhance the distribution of induction heating in the system.

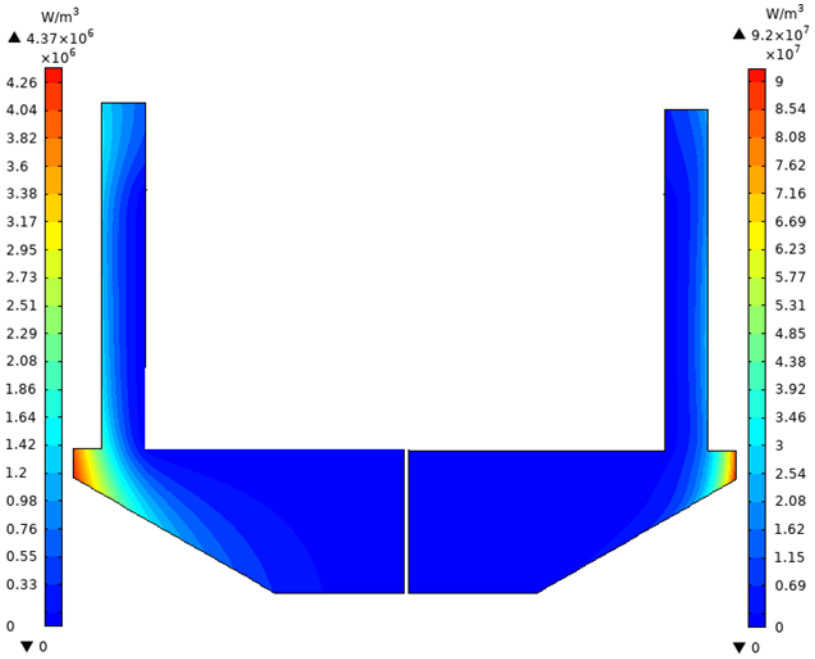

Fig. 3. Heat distribution in the crucible for Case 1 (on the right side) and Case 2 (on the left side).

Table 3. Input Flow and Heat Generated in the System (W)

Electrical conductivity of the coil (s/m)	Input current to the coil (A)	The heat generated in the coil (W)	The heat generated in the melt (W)	Total heat generated in the system (W)
70000	482	15914 (90%)	261 (2%)	17696
151	1264	1513 (6%)	13150 (50%)	26171

In the CZ growth system, fluid flow is crucial. It was found that the electrical conductivity of the crucible does not directly influence the argon gas flow during growth (Fig. 4). Argon gas flow is mainly controlled by external factors

such as gas pressure, nozzle design, and growth configuration. In the CZ crystal growth method, argon gas is typically used as a protective atmosphere to prevent oxidation of the melt and ensure a stable thermal environment. The gas flow is adjusted to create a controlled atmosphere around the melt and crystal, ensuring a stable growth environment. While the electrical conductivity of the crucible indirectly affects temperature distribution and heat transfer, it does not have a direct impact on the argon gas flow in the CZ crystal growth process.

Fig. 5 shows the flow distribution of molten germanium for both Cases 1 and 2. As the electrical conductivity of the crucible increases, the melt flow in the system also increases. In Case 1, two vortices are formed in the melt. These consist of a large lower vortex due to natural convection and a vortex beneath the free surface of the melt. In the lower vortex, the flow moves upward along the walls of the crucible due to the heating of the melt by the side wall of the crucible. The flow in the upper vortex moves radially outward along the surface of the melt, becomes denser due to cooling, and then flows downward again. In Case 2, due to non-uniform temperature distribution in the melt, the upper vortex becomes weaker, and there is a relatively larger lower vortex.

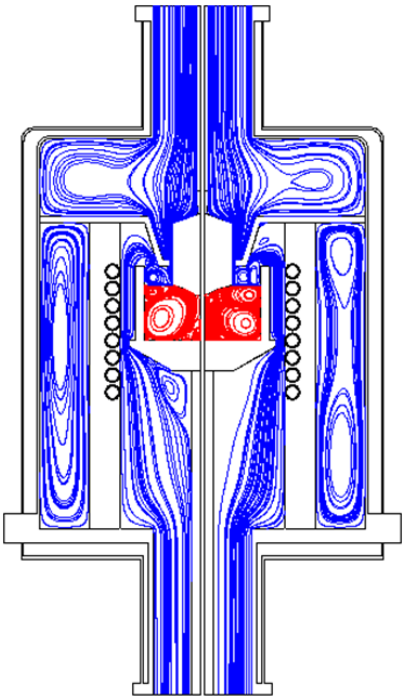

Fig. 4. Flow distribution in the growth system in Case 1 (right hand side) and in Case 2 (left hand side).

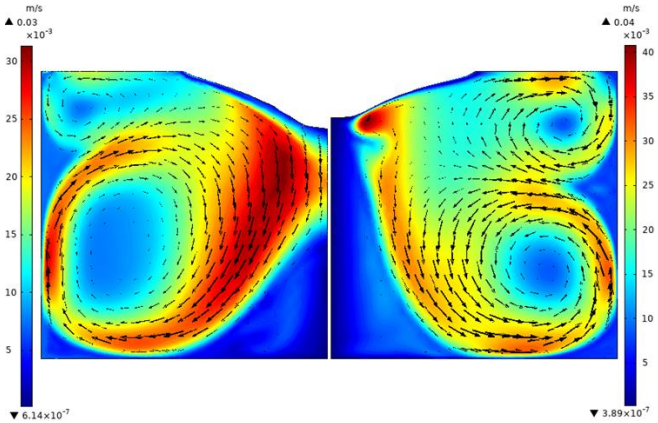

Fig. 5. Flow distribution in the melt in Case 1 (right hand side) and Case 2 (left hand side).

3.2. Thermal Field

Fig. 6 illustrates the impact of temperature-dependence of crucible electrical conductivity on the temperature distribution in the growth system. The direction of gas convection significantly affects the temperature gradient in the system. Isotherm lines in the growth system exhibit curvature proportional to the structure and gas flow intensity. They are pushed from the upper part of the system along the gas flow, which is proportional to its velocity, and diverted towards the channels and lower outlets. A reduction in electrical conductivity (Case 2) leads to an increase in the input electric current, and consequently, an increase in the heat generated in the growth system. As a result, the temperature boundary layers expand along the joint region of the crucible/gas towards the lower parts of the system with higher temperatures compared to Case 1.

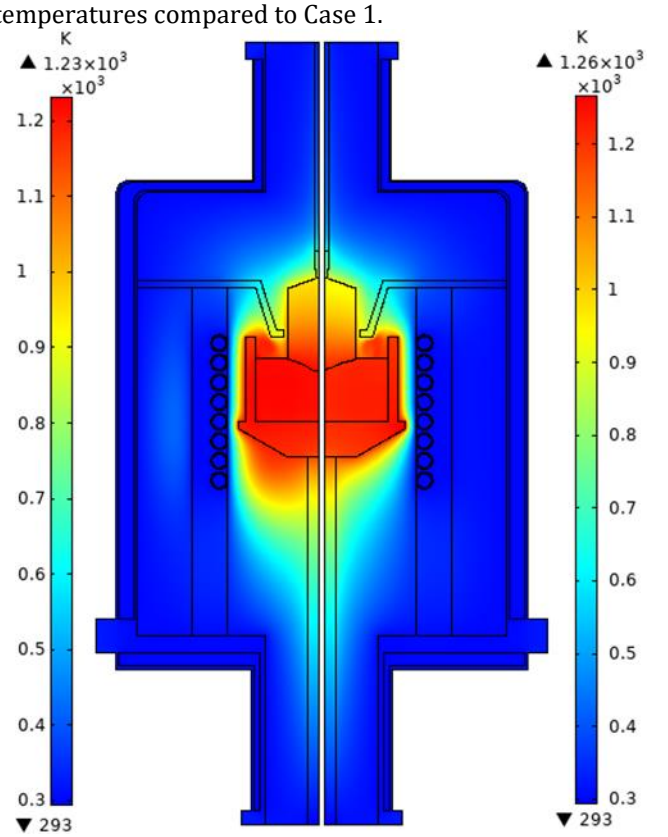

Fig. 6. Temperature distribution of the growth system in Case 1 (right hand side) and Case 2 (left hand side).

When an electric current flows through a conductive material, it produces heat through Joule heating. The material's electrical conductivity determines its efficiency in conducting this heat. A material with higher electrical conductivity can distribute heat more evenly, resulting in a uniform temperature distribution in the melt (Case 1). Conversely, a material with lower electrical conductivity may experience localized hotspots, causing uneven heat fields (Case 2). The material's electrical conductivity also impacts its heat dissipation ability. A material with higher electrical conductivity can more effectively transfer heat to the surrounding environment, leading to improved heat dissipation. This contributes to maintaining a more stable and controlled thermal field in the crystal growth system.

Additionally, the material's electrical conductivity affects the flow intensity and distribution in the thermal field of the melt. Higher electrical conductivity can contribute to a more stable and controlled temperature gradient, impacting the uniformity of the thermal field and, consequently, the consistency of crystal growth and reduction of temperature-related defects. Figure 7(a) illustrates a uniform temperature distribution in Case 1, whereas solidification occurs at the bottom of the melt. This problem can be resolved by moving the crucible.in Case 2.

3.3. Melt-Crystal Interface

The crucible's ability to conduct heat depends on its electrical conductivity. A crucible with high electrical conductivity can distribute heat more efficiently, resulting in a more uniform temperature distribution in the melt. This, in turn, can lead to a more stable interface between the melt and the crystal, ultimately improving crystal growth. In Figure 8, the shape of melt-crystal interface for a crystal height of 10 cm is shown for both cases. The results indicate that in Case 2, the penetration of the germanium crystal into the melt increases, resulting in a more convex crystal-melt interface being observed. This is due to non-uniform temperature distribution in the melt caused by the lower conductivity of the crucible. In Case 1, the depth of the crystal immersed in the melt is 14.5 mm, whereas in Case 2, it is 17.98 mm.

3.4. Thermal stress and dislocation density in the grown crystal

It is important to note that the electrical conductivity of the crucible is just one of several factors that can affect the von Mises stress and dislocation density in CZ germanium crystal. Other parameters such as temperature gradient, pulling speed, and crystal growth conditions also play a crucial role in determining the final crystal quality. Higher electrical conductivity can lead to more efficient heat dissipation from the crucible, reducing the temperature gradient and thermal stress in the crystal. Lower thermal stress can help minimize dislocation formation and reduce the likelihood of crystal cracking. In Case 1, due to the presence of a higher temperature gradient at the two ends of the grown crystal, we will observe an increase in maximum stress compared to Case 2 (Figure 9(a)).

The maximum dislocation density in lower electrical conductivity is higher, and since the maximum dislocation density is in the crystal neck and what matters is the body of the crystal, one can see an increase in dislocation distribution values along the crystal wall during the growth of the crystal with increasing electrical conductivity of the crucible. Therefore, due to the presence of a higher temperature gradient along the length of the crystal in Case 1, the stress and dislocation fields along the crystal wall in this case are higher compared to Case 2.

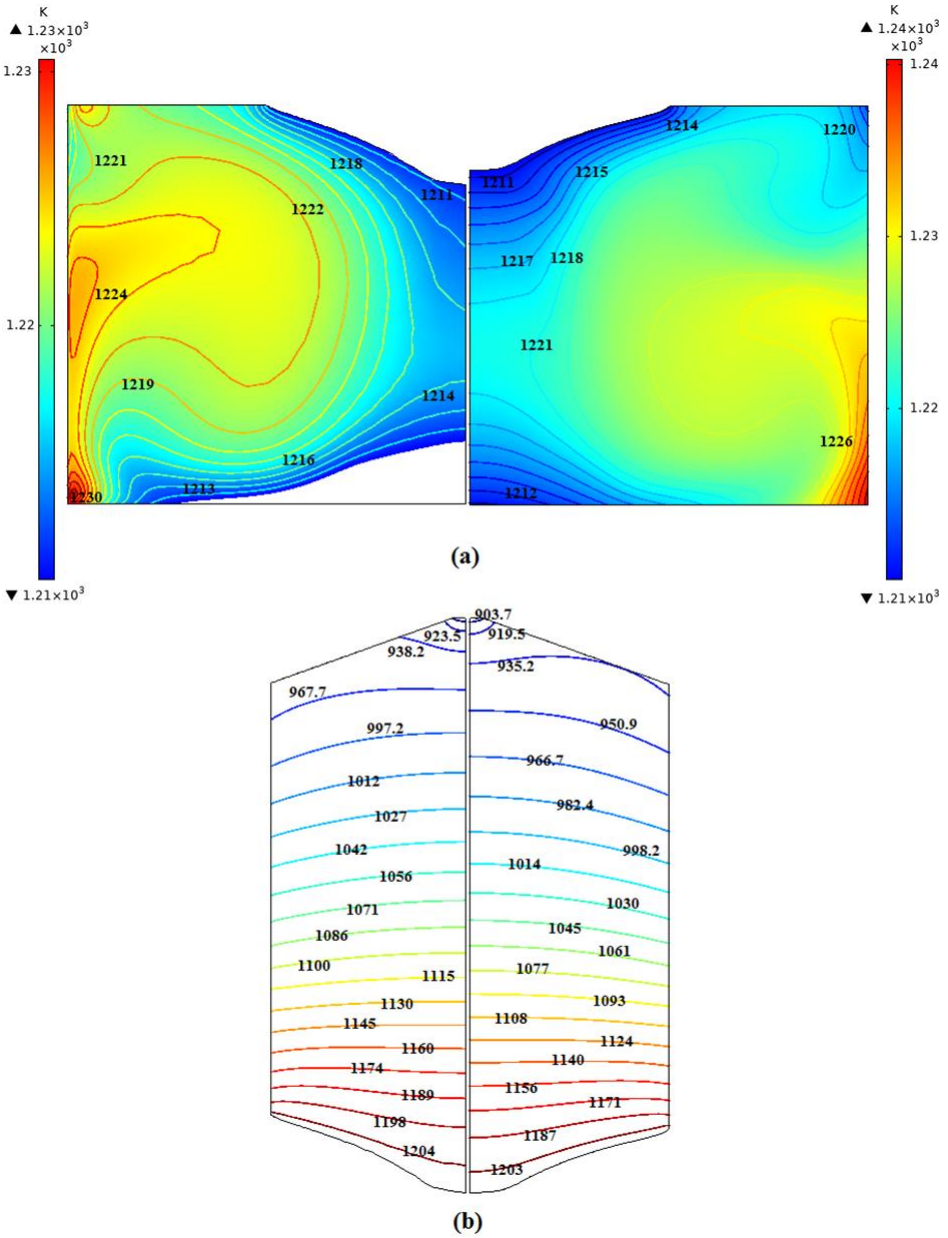

Fig. 7. Temperature distribution in the (a) melt and (b) crystal for Case 1 (right hand side) and Case 2 (left hand side).

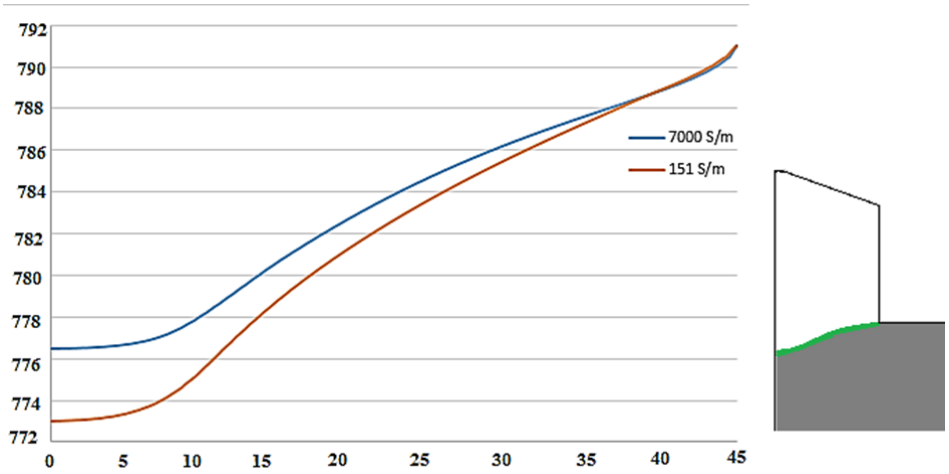

Fig. 8. The shape of melt-crystal interface, for 10 cm crystal in Case 1 (blue diagram) and Case 2 (red diagram).

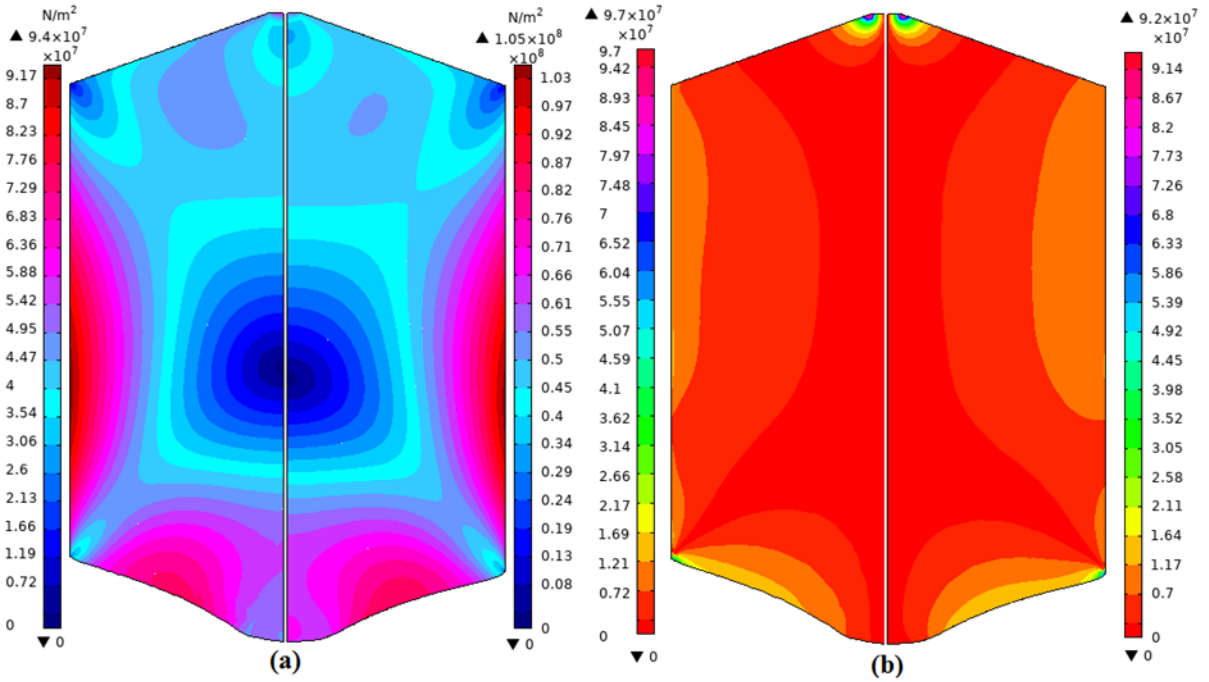

Fig. 9. Distribution of (a) Thermal stress and (b) Dislocation density in one-centimeter crystal for Case 1 (right hand side) and Case 2 (left hand side).

4. Conclusion

The electrical conductivity of the crucible in the germanium Czochralski growth system significantly impacts crystal growth. It directly influences induction heating, temperature distribution, and heat dissipation, affecting the uniformity of the thermal field and the melt-crystal interface. Additionally, it minimizes stress and dislocation in the grown crystal, ultimately influencing the quality of the final product. Higher electrical conductivity leads to more efficient heat dissipation, reduced stress, and lower dislocation, contributing to improved crystal quality.

Acknowledgements

There is nothing to acknowledgement.

Conflicts of Interest

The author declares that there is no conflict of interest regarding the publication of this article.

References

[1] Depuydt, B., Theuwis, A. and Romandic, I., 2006. Germanium: From the first application of Czochralski crystal growth to large diameter dislocation-free wafers. *Materials Science in Semiconductor Processing*, *9*(4-5), pp.437-443.

[2] Patidar, B., M. Hussain, M., Jha, S.K., Sharma, A. and Tiwari, A.P., 2017. Analytical, numerical and experimental analysis of induction heating of graphite crucible for melting of non-magnetic materials. *IET Electric Power Applications*, *11*(3), pp.342-351.

[3] Miller, W., Abrosimov, N., Fischer, J., Gybin, A., Juda, U., Kayser, S. and Janicskó-Csáthy, J., 2019. Quasi-transient calculation of Czochralski growth of Ge crystals using the software elmer. *Crystals*, *10*(1), p.18.

[4] Gresho, P.M. and Derby, J.J., 1987. A finite element model for induction heating of a metal crucible. *Journal of crystal growth*, *85*(1-2), pp.40-48.

[5] Derby, J.J., Atherton, L.J. and Gresho, P.M., 1989. An integrated process model for the growth of oxide crystals by the Czochralski method. *Journal of crystal growth*, *97*(3-4), pp.792-826.

[6] Chen, Q.S., Zhang, H., Prasad, V., Balkas, C.M. and Yushin, N.K., 2001. Modeling of heat transfer and kinetics of physical vapor transport growth of silicon carbide crystals. *J. Heat Transfer*, *123*(6), pp.1098-1109.

[7] Jing, C.J., Kobayashi, M., Tsukada, T., Hozawa, M., Fukuda, T., Imaishi, N., Shimamura, K. and Ichinose, N., 2003. Effect of RF coil position on spoke pattern on oxide melt surface in Czochralski crystal growth. *Journal of crystal growth*, *252*(4), pp.550-559.

[8] Du, D.X. and Munakata, T., 2005. Temperature distribution in an inductively heated CZ crucible. *Journal of crystal growth*, *283*(3-4), pp.563-575.

[9] Kirpo, M., 2013. Global simulation of the Czochralski silicon crystal growth in ANSYS FLUENT. *Journal of crystal growth*, *371*, pp.60-69.

[10] Tavakoli, M.H., Renani, E.K., Honarmandnia, M. and Ezheiyan, M., 2018. Computational analysis of heat transfer, thermal stress and dislocation density during resistively Czochralski growth of germanium single crystal. *Journal of Crystal Growth*, *483*, pp.125-133.

[11] Saadatirad, M., Tavakoli, M.H., Khodamoradi, H. and Masharian, S.R., 2021. Effect of the pulling, crystal and crucible rotation rate on the thermal stress and the melt–crystal interface in the Czochralski growth of

germanium crystals. *CrystEngComm*, *23*(39), pp.6967-6976.
[12] Semiatin, S.L., 1988. *Elements of induction heating: design, control, and applications*. Asm International.
[13] Rudnev, V., Loveless, D. and Cook, R.L., 2017. *Handbook of induction heating*. CRC press.
[14] Leatherman, A.F. and Stutz, D.E., 1969. *Induction Heating Advances: Applications to 5800° F* (Vol. 5071). Technology Utilization Division, National Aeronautics and Space Administration.
[15] Tavakoli, M.H. and Karbaschi, H., 2021. Numerical study of influences of the input current frequency on the induction heating process. *Progress in Physics of Applied Materials*, *1*(1), pp.44-49.
[16] Tavakoli, M.H., Karbaschi, H. and Samavat, F., 2009. Computational modeling of induction heating process. *Progress in Electromagnetics research letters*, *11*, pp.93-102.